Engineered *Escherichia coli* platforms for tyrosine-derivative production from phenylalanine using phenylalanine hydroxylase and tetrahydrobiopterin-regeneration system

Yasuharu Satoh [1,2*], Keita Fukui [3], Daisuke Koma [4], Ning Shen [2], and Taek Soon Lee [5]

[1] Faculty of Engineering, Hokkaido University, Sapporo 060-8628, Japan.

[2] Graduate School of Chemical Sciences and Engineering, Hokkaido University, Sapporo 060-8628, Japan.

[3] Ajinomoto Co., Inc., Tokyo 104-8315, Japan.

[4] Osaka Research Institute of Industrial Science and Technology, Osaka 536-8553, Japan.

[5] Biological Systems and Engineering Division, Lawrence Berkeley National Laboratory, Berkeley, CA 94720, USA.

*Corresponding author: Tel. & Fax: +81 11 706 7118, E-mail: syasu@eng.hokudai.ac.jp

ABSTRACT

Background: Aromatic compounds derived from tyrosine are important and diverse chemicals that have industrial and commercial applications. Although these aromatic compounds can be obtained by extraction from natural producers, their growth is slow, and their content is low. To overcome these problems, many of them have been chemically synthesized from petroleum-based feedstocks. However, because of the environmental burden and depleting availability of feedstock, microbial cell factories are attracting much attention as sustainable and environmentally friendly processes.

Results: To facilitate development of microbial cell factories for producing tyrosine derivatives, we developed simple and convenient tyrosine-producing *Escherichia coli* platforms with a bacterial phenylalanine hydroxylase, which converted phenylalanine to tyrosine with tetrahydromonapterin as a cofactor, using a synthetic biology approach. By introducing a tetrahydrobiopterin regeneration system, the tyrosine titer of the plasmid-based engineered strain was 4.63 g/L in a medium supplemented with 5.00 g/L phenylalanine with a test tube. The strains were successfully used to produce industrially attractive compounds, such as tyrosol with a yield of 1.58 g/L by installing a tyrosol-producing module consisting of genes encoding tyrosine decarboxylase and tyramine oxidase on a plasmid. Gene integration into *E. coli* chromosomes has an advantage over

the use of plasmids because it increases genetic stability without antibiotic feeding to the culture media and enables more flexible pathway engineering by accepting more plasmids with artificial pathway genes. Therefore, we constructed a plasmid-free tyrosine-producing platform by integrating five modules, comprising genes encoding the phenylalanine hydroxylase and tetrahydrobiopterin regeneration system, into the chromosome. The platform strain could produce 1.04 g/L of 3,4-dihydroxyphenylalanine, a drug medicine, by installing a gene encoding tyrosine hydroxylase and the tetrahydrobiopterin regeneration system on a plasmid. Moreover, by installing the tyrosol-producing module, tyrosol was produced with a yield of 1.28 g/L.

Conclusions: We developed novel *E. coli* platforms for producing tyrosine from phenylalanine at multi-gram-per-liter levels in test-tube cultivation. The platforms allowed development and evaluation of microbial cell factories installing various designed tyrosine-derivative biosynthetic pathways at multi-grams-per-liter levels in test tubes.

Keywords: Phenylalanine hydroxylase, tyrosine, tetrahydrobiopterin, chromosome engineering, hydroxytyrosol.

BACKGROUND

Aromatic compounds are an important class of diverse chemicals with a wide range of industrial and commercial applications, such as nutraceuticals (vitamin E, resveratrol, hydroxytyrosol), pharmaceuticals (3,4-dihydroxyphenylalanine [DOPA], adrenalin, morphine, melatonin), fragrance ingredients (2-phenylethanol, 3-phenylpropanol), and polymers (styrene, hydroxystyrene, tyrosol) **[1–6]**. These compounds can be produced by various plants, algae, fungi, and bacteria from proteinogenic amino acids, with phenylalanine (Phe), tyrosine (Tyr), and tryptophan (Trp) as precursors.

Although these aromatic compounds can be obtained by extraction from producers, their growth is slow. Additionally, the content of the compounds is low. To overcome these problems, many aromatic compounds have been chemically synthesized from petroleum-based feedstocks. However, because of the environmental burden and depleting availability of feedstock, other sustainable and environmentally friendly processes are required.

Recent remarkable advances in metabolic engineering and synthetic biology have made it possible to develop fermentative processes using microbial cell factories, which utilized natural and non-natural biosynthetic pathways to produce chemicals from renewable resources **[7, 8]**. Aromatic compounds derived from Tyr are important

chemicals and various microbial cell factories that produce Tyr derivatives have been developed by already-known and artificially designed biosynthetic pathways that utilize enzymes/genes from different sources **[9–11]**. *Escherichia coli* and yeast have been extensively used as hosts **[1–4]**. Several bacteria were also considered. Among the hosts, *E. coli* exhibits considerable advantages in the rapid development of microbial cell factories suitable for industrial production because of its high growth rate and well-studied genome and metabolic network as well as the availability of various synthetic biology tools for engineering and established strategies for high-cell-density fermentation in inexpensive media **[5]**.

We have succeeded in engineering *E. coli* to produce DOPA, tyrosol, and hydroxytyrosol from Tyr, which was supplied via a central metabolic pathway and supplemented in cultivation media; however, the titers were low (<1.22 mM) (Figure 1A) **[12, 13]**. Therefore, for high Tyr-derivative production, enhancement of Tyr supply in *E. coli* is needed. However, Tyr production by *E. coli* is limited because its biosynthesis is elaborately regulated **[14]**. Furthermore, low solubility of Tyr (0.45 g/L [2.5 mM] in water at 25 °C) makes it difficult to feed Tyr into culture broths at high concentrations **[15]**. To increase Tyr supply, various metabolic engineering approaches, such as deregulation at transcriptional level and overexpression of bottleneck and feedback-resistant enzymes,

have been employed **[16–18]**. Although the titers by flask-scale production were reported to be 2 to 3 g/L by the rationally engineered strains, further enhanced production is necessary for industrial applications.

Tyr can be converted from Phe by Phe hydroxylase (PheH) **[19, 20]**. PheH is an iron-dependent non-heme enzyme that catalyzes *para*-hydroxylation of Phe using O_2 and tetrahydrobiopterin (BH4) as the reducing substrate (Figure 1A). Some bacteria, including *Chromobacterium*, *Pseudomonas*, and *Xanthomonas* species, have PheHs, which use tetrahydromonapterin (MH4) instead of BH4 as the cofactor **[21, 22]**. Previously, we succeeded in engineering an *E. coli* strain that could oxidize Tyr to DOPA using mouse Tyr hydroxylase (TyrH), a PheH homolog, and endogenous MH4, together with the human BH4 regeneration system, which reduces the oxidized form of the cofactor, quinonoid dihydromonapterin (qMH2) **[13]**. In this study, we developed a simple and convenient Tyr-supplying *E. coli* strain by utilizing a bacterial PheH and the human BH4 regeneration system. The Tyr titer of the strain expressing these enzymes with a plasmid was 4.63 g/L (25.5 mM) by feeding 5.00 g/L (30.3 mM) of Phe, a highly water-soluble compound (29.6 g/L [179 mM] in water at 25 °C). To enable more flexible pathway engineering, we also constructed a plasmid-free platform, which was performed by integration of the above-mentioned genes of the PheH and the human BH4

regeneration system into the chromosome. This has an advantage over the use of plasmids because it increases genetic stability without antibiotic feeding into the culture media and accepts more plasmids carrying artificial pathway genes. These platform strains were successfully applied to produce Tyr-derived compounds, such as DOPA, tyrosol, and hydroxytyrosol.

RESULTS

Screening of PheHs for Tyr-overproduction.

We searched for PheHs with high activities for construction of an *E. coli* platform to produce Tyr from Phe at a high titer. First, the activity of rat PheH (RatPheH) was examined because the enzyme is well characterized and has been successfully expressed as an active form in *E. coli* **[19, 23]**. The RatPheH consists of *N*-termins regulatory domain and *C*-terminus catalytic domain. A truncated enzyme lacking the regulatory domain was previously reported to have almost the same activity as the parental enzyme and to be highly expressed in *E. coli*. Therefore, a codon-optimized DNA fragment encoding only the catalytic domain of the RatPheH (RatPheHc) was synthesized and cloned into the protein expression vector pQE1a-Red (pQE1a-RatC, Table 1, supplementary materials), in which the gene was expressed under the control of the strong

127 *tac* promoter and repressed by *lac* operator and *lac* repressor (LacI). To estimate the net
128 effect of PheH activity for Tyr production, a Tyr-auxotrophic mutant *E. coli* Y0 strain, in
129 which *tyrA* encoding bifunctional chorismate mutase/prephenate dehydratase was
130 knocked out **[24]**, was used as host (Table 2, supplementary materials). For regeneration
131 of the cofactor MH4, which is stoichiometrically consumed during the Phe hydroxylation
132 reaction, the human pterin-4α-carbinolamine dehydratase gene (*PCD*) and
133 dihydropteridine reductase gene (*DHPR*) were also coexpressed, in that order, under the
134 control of a *lac* promoter using plasmid pSTV-BH4R (Figure 1B). The production of the
135 PCD and DHPR was confirmed by Western blot analyses (Figure S1) and the strain Y0
136 harboring pSTV-BH4R was designated as strain YBR (Table 2).
137 Then, the RatPheHc expression in strain YBR, harboring pQE1a-RatC, was analyzed
138 by sodium dodecyl sulfate-polyacrylamide gel electrophoresis (SDS-PAGE). As shown
139 in Figure S2, soluble expression of the RatPheHc was confirmed. To examine Tyr
140 production, the transformant was cultured in M9Y medium, including 30.3 mM (5.00
141 g/L) Phe and 1.0%(w/v) glucose, for 48 h in test tubes, and the product was analyzed by
142 high-performance liquid chromatography (HPLC). As shown in Figure 2A,
143 approximately 0.443 ± 0.030 mM (0.080 g/L) of Tyr was produced even though nearly
144 all Phe remained. Therefore, we tried to improve the low conversion rate.

145 The oxidized form of cofactor qMH2 generated during the Phe hydroxylation
146 reaction is reduced by DHPR with NADH. Glycerol reportedly regenerates NADH more
147 effectively than glucose **[25]**; thus, glycerol was used as the sole carbon source. Although
148 the Tyr titer was improved to 1.09 ± 0.19 mM (0.197 g/L), most of the Phe still remained
149 in the culture medium (Figure 2B). In addition, after 24 h of cultivation, cell growth was
150 slower than when glucose was used as carbon source.

151 To further improve the productivity, we next examined the activities of seven other
152 bacterial PheHs. The genes were selected from different classes of bacteria, including
153 *Bacillus* sp. INT005 (*BsPheH*) **[26]** from Bacilli; *Cupriavidus necator* (*CnPheH*),
154 *Chromobacterium violaceum* (*CvPheH*) and *Gulbenkiania* sp. SG4523 (*GsPheH1* and
155 *GsPheH2*) from β-proteobacteria; and *Xanthomonas oryzae* (*XoPheH*) and *Pseudomonas*
156 *putida* (*PpPheH*) from γ-proteobacteria. The identities of PheHs among these enzymes
157 are 20% to 70% (Table S1). Polymerase chain reaction (PCR) amplified-DNA fragments
158 encoding PheHs were cloned into the protein expression vector pQE1a-Red and used for
159 Tyr production in the same manner as described above. As shown in Figure S2, we
160 confirmed that all enzymes were produced as soluble forms in the strain YBR by SDS-
161 PAGE analysis. In terms of Tyr production (Figures 3A and 3B), a strain YBR carrying
162 *GsPheH1* yielded the highest titer (24.7 ± 1.3 mM [4.48 g/L]) among the tested PheHs at

48 h of cultivation. Therefore, *GsPheH1* was selected for further analyses.

Plasmid-based Tyr-producing platform

Construction of plasmid-based Tyr-producing platform

To construct pathways for Tyr-derivative production, many pathway genes are introduced into the host cell. From this point of view, the number of plasmids carrying genes encoding PheH and co-factor regeneration enzymes should be minimal. Therefore, we constructed plasmid pQE1a-Gs1-BH4R (Figure 1B and Table 1), which co-expresses *GsPheH1* and the BH4-regeneration genes, which encode PCD and DHPR, as described in supplementary materials. As shown in Figure 3C, strain Y0 harboring pQE1a-Gs1-BH4R, designated as strain PGs (Table 2), converted most of the Phe to Tyr, 25.5 ± 1.6 mM (4.63 g/L) after 48 h of cultivation. The cell growth and Tyr titer (24.2 ± 1.7 mM [4.39 g/L]) at 24 h of cultivation were markedly improved when compared with those of strain YBR harboring pQE1a-Gs1 (Figure 3B). Therefore, we then applied strain PGs for Tyr-derivative production.

Application of a plasmid-based Tyr-producing platform strain

We evaluated the above-mentioned plasmid-based Tyr-producing platform by

181 measuring tyrosol productivity. Tyrosol is an attractive phenolic compound used for
182 pharmaceuticals and fine chemicals **[27–29]**. We have constructed a tyrosol biosynthetic
183 pathway from Tyr via three steps: decarboxylation of Tyr to tyramine, deamination of
184 tyramine to 4-hydroxyphenylacetaldehyde (HPAAld), and reduction of HPAAld to
185 tyrosol (Figure 1A) **[12]**. As endogenous enzyme(s) in *E. coli*, such as alcohol
186 dehydrogenase(s), can catalyze the reduction of HPAAld to tyrosol, two genes encoding
187 Tyr decarboxylase (TDC) from *Papaver somniferum* and tyramine oxidase (TYO) from
188 *Micrococcus luteus* were introduced into the Tyr producer. We previously constructed a
189 plasmid, pBbS1a-2, which carried the TDC- and TYO-encoding genes, but the selection
190 marker was ampicillin-resistance (Ap^R), which is the same as pQE1a-Gs1-BH4R. We
191 therefore reconstructed plasmids with a pCF1s-Red vector (streptomycin-resistance
192 marker [Sm^R], pCDF ori) as described in supplementary materials. The TDC- and TYO-
193 encoding genes were cloned as artificial operons into pCF1s-Red, so that the order of the
194 two genes was interchanged to make pCF1s-TDC-TYO and pCF1s-TYO-TDC,
195 respectively (Figure 1B). When the transformants were cultured in M9Y medium with
196 30.3 mM (5.00 g/L) Phe for 72 h at 30 ºC, tyrosol was produced with a yield of 4.93 ±
197 0.31 mM (0.682 g/L) by strain PGs harboring pCF1s-TYO-TDC, while 11.5 ± 1.2 mM
198 (1.58 g/L) was yielded by strain PG harboring pCF1s-TDC-TYO, which is 2.3-fold higher

than that of the former strain (Figure 4A and 4B). The results suggested that the gene order in the operon was crucial for increased titer. Thus, we demonstrated that the platform could be applicable for Tyr-derivative-producing pathways.

Plasmid-free Tyr-producing platform

Integration of Tyr-producing module into E. coli *chromosome*

Gene integration into the *E. coli* chromosome offers considerable advantages over the use of plasmids, especially for large scale industrial applications **[18, 30]**. It increases genetic stability without antibiotic feeding of the culture media and enables more flexible pathway engineering as more plasmids carrying artificial pathway genes are acceptable. Therefore, we attempted to develop a plasmid-free Tyr-supplying platform *E. coli* strain by integrating *GsPheH1* and BH4-regeneration-related genes into the chromosome as a cassette (Tyr-producing module).

For integration of the Tyr-producing module into the *E. coli* chromosome, we employed the bacteriophage λRed recombineering system **[31–33]**. As an integration site, we selected the *tyrA* locus because the *tyrA*-knockout mutant Y0 could be recovered by introduction of *GsPheH1* and BH4-regeneration-related genes as described above. As described in supplementary materials, the desired strain GsBR1 was successfully

obtained and then evaluated for its Tyr production (Figure 5). When cultivated under the same conditions mentioned above, Tyr productivity was markedly decreased, to 0.252 ± 0.012 mM (0.046 g/L), when compared with that of the plasmid-based strain PGs (Figure 3C). Considering that the copy number of pQE vectors used for the plasmid-based platform is 20 to 30 (Qiagen, Dusseldorf, Germany), the low productivity was likely due to gene dosage of the Tyr-producing module.

To improve Tyr productivity, the module was additionally integrated into the *feaB–tynA* region of strain GsBR1 because the region was already knocked out. We obtained the strain by the method described in the supplementary materials and it was designated as strain GsBR2. The Tyr titer of the constructed strain was slightly enhanced to 0.705 ± 0.023 mM (0.128 g/L), compared to that of strain GsBR1 (Figure 5), but was still lower than that of the plasmid-based strain PGs.

Stepwise and scarless integration of the Tyr-supplying module at different locations of the chromosome using λRed recombinase

As demonstrated with the construction of the strains, GsBR1 and GsBR2, λRed recombineering is a powerful tool for integration of a DNA fragment prepared by PCR into the desired chromosomal site of *E. coli*. In general, an antibiotic-resistance marker is

repeatedly used for gene integration and knockout and is removed with flippase (FLP)/FLP recognition target (FRT) recombination for marker recycling **[32, 33]**. However, multiple FRT-sequences (scars) left on the chromosome can induce chromosomal deletion and rearrangements between undesired FRT-sequences in the FLP/FRT recombination reaction. We therefore attempted to develop a genome-engineering method without scar sequences based on λRed-based recombineering and auxotrophy complementation. The scheme depicting our process is shown in Figure 6. At first, an essential gene for *E. coli* was selected as the target locus for module integration and its knockout mutant was constructed by the λRed-mediated recombination method, using an appropriate antibiotic-resistance gene. The auxotrophic mutant was then transformed with λRed recombinase and the DNA fragment assembled the essential gene, the target module, and attached homology arms for chromosome integration. Finally, DNA integration in recombinant cells showing recovery of the auxotrophic phenotype was confirmed by PCR and sequence analysis. To reduce unexpected effects on downstream genes by the module integration, we selected essential genes that were least likely to form an operon structure with downstream genes.

To examine the effectivity of this strategy, *aroD* (3-dehydroquinate dehydratase gene), essential for aromatic amino acid production **[24, 34]**, was targeted. A DNA

253 fragment, comprised *aroD* and the Tyr-producing module, was replaced with the
254 kanamycin (Km)-resistance marker in the chromosome of an *aroD*-knockout mutant
255 which was derived from strain GsBR2 (strain GsBR2Δ*aroD*) as described in
256 supplementary materials. After selection in the M9 minimal medium, we successfully
257 obtained a recombinant strain (GsBR3). Furthermore, the Tyr-producing module was also
258 integrated downstream of *cysE* (serine *O*-acetyltransferase gene) and *serA* (3-
259 phosphoglycerate dehydrogenase gene), in the same manner as for *aroD*, to construct
260 strains GsBR4 and GsBR5, respectively (supplementary materials). As shown in Figure
261 5, depending on the number of the Tyr-producing modules, Tyr production by strains
262 GsBR3 to GsBR5 after 48 h of cultivation was almost linearly enhanced up to 3.23 ± 0.09
263 mM (0.586 g/L), which was approximately 13-fold higher than that of strain GsBR1.
264 However, the titer of strain GsBR5 was merely 12.6% of that of strain PGs.
265
266 ***Application of plasmid-free Tyr-producing platform for its derivatives production***
267 We next evaluated the plasmid-free platform based on DOPA and tyrosol production.
268 We first examined the production of DOPA, which is used as a drug for treatment of
269 Parkinson's disease **[35]**. We previously reported that DOPA was produced from Tyr in *E.*
270 *coli* expressing the mouse TyrH-encoding gene together with human BH4-regeneration-

271 related genes on the pBbE1k-3 plasmid **[13]**. We therefore used this plasmid, which
272 included *TyrH*, *DHPR*, and *PCD* as an operon in this order, under the control of *trc*
273 promoter (DOPA-producing module). The DOPA productivity of transformant of strain
274 GsBR5 harboring pBbE1k-3 (Figure 7A) was 5.28 ± 0.04 mM (1.04 g/L), demonstrating
275 that strain GsBR5 can be used to produce DOPA. Interestingly, the titer exceeded Tyr
276 production (3.23 mM) of the host strain GsBR5, suggesting that the BH4-regeneration
277 system, additionally introduced by the plasmid pBbE1k-3, elevated Tyr production. To
278 investigate this speculation, Tyr production of strain GsBR5 harboring pSTV-BH4R was
279 examined (Figure 5). As expected, the titer was markedly increased and reached 15.8 ±
280 0.5 mM (2.86 g/L) after 48 h of cultivation. In contrast, additional GsPheH1 expression
281 was poorly effective for Tyr production (Figure 5). Taken together, the cofactor
282 regeneration step is a bottleneck in strain GsRB5.

283 Next, we evaluated tyrosol production using pCF1s-TDC-TYO. This transformant of
284 strain GsBR5 produced 4.41 ± 0.20 mM (0.609 g/L) tyrosol at 72 h. Furthermore, strain
285 GsBR5 harboring pCF1s-TDC-TYO-BH4R, a derivative of pCF1s-TDC-TYO that had
286 the BH4-regeneration genes inserted to improve the rate-limiting step of the host strain,
287 produced 2.1-fold more tyrosol (9.27 ± 0.64 mM [1.28 g/L]) (Figure 7B), which was
288 comparable to that of the plasmid-based platform with strain PGs harboring pCF1s-TDC-

289 TYO (11.5 mM), indicating that the additional introduction of the BH4-regeneration
290 system was effective for increased production.

291 Furthermore, we attempted to convert strain GsBR5 harboring the DOPA-producing
292 module to hydroxytyrosol-producing cells. Hydroxytyrosol is a powerful antioxidant and
293 used for human health promotion **[36, 37]**. Hydroxytyrosol is obtained from DOPA by
294 three steps similar to those involved in tyrosol production; decarboxylation of DOPA,
295 deamination of dopamine, and reduction of 3,4-dihydroxyphenylacetaldehyde
296 (DHPAAld, Figure 1A) **[13]**. For specific production of hydroxytyrosol without
297 byproducts, a DOPA-specific decarboxylase (DDC) from *Sus scrofa,* which does not
298 recognize Tyr **[38]**, was used. Since hydroxytyrosol is obtained from dopamine by TYO
299 from *M. luteus,* and endogenous alcohol dehydrogenase(s) in *E. coli*, the already-
300 constructed plasmid pBbS1a-3, which includes the genes encoding DDC and TYO as an
301 operon in this order under the control of a *trc* promoter (hydroxytyrosol-producing
302 module), was used. Strain GsBR5 harboring pBbE1k-3 and pBbS1a-3 was cultured using
303 the same procedures described above. As shown in Figure 8, 0.147 ± 0.015 mM (0.023
304 g/L) hydroxytyrosol was produced. This titer was rather low, considering that DOPA
305 production of strain GsBR5 harboring pBbE1k-3 was 5.28 ± 0.04 mM (1.04 g/L, Figure
306 7A). Since growth inhibition of GsBR5 harboring pBbE1k-3 and pBbS1a-3 was observed

(Figure S3), additional expression of *DDC* and *TYO* would negatively affect the cell growth. Therefore, we cultivated the strain under various conditions by varying isopropyl-β-D-thiogalactopyranoside (IPTG) concentrations. Consequently, growth inhibition was relieved depending on a decrease in IPTG concentration (Figure S3). The titer of hydroxytyrosol production was also enhanced to 0.253 ± 0.006 mM (0.039 g/L) by addition of 100 μM IPTG (Figures 8). Thus, strain GsBR5 could be applied to develop microbial cell factories with multi-modules for Tyr-derivative production.

DISCUSSION

In this study, we reported novel *E. coli* platforms for producing Tyr from Phe, using *Gulbenkiania* sp. PheH1 together with human BH4-regeneration system, at multi-gram-per-liter levels in test-tube cultivation. The titer of our engineered strain using a plasmid (strain PGs) was higher than those of rationally engineered Tyr-overproducing strains in flask cultivation (3.0 g/L, 16.6 mM) **[17]**. In addition, our developed platform strains were successfully applied for producing industrially valuable aromatic compounds, DOPA, tyrosol, and hydroxytyrosol, and the titers were improved, compared to those previously reported **[12, 13]**. Furthermore, we successfully optimized the tyrosol-producing module and revealed a bottleneck step in the hydroxytyrosol-producing pathway. Therefore, the

325 engineered strains would be useful for the efficient development of already known and
326 artificially designed biosynthetic pathways. Moreover, this would enable us easy access
327 to adequate amount of rare natural Tyr-derivatives for further analysis.

328 In terms of hydroxytyrosol production, the titer of strain GsBR5 as a host (0.253 mM,
329 0.039 g/L) was improved compared with that (0.19 mM, 0.029 g/L) of *E. coli* Δ*feaB* with
330 both DOPA- and hydroxytyrosol-producing modules in cultures fed 1 mM Tyr **[13].**
331 However, it was quite low, considering that the strain GsBR5 with the DOPA-producing
332 module produced 5.28 mM (1.04 g/L) of DOPA. Recently, Nakagawa *et al*. reported that
333 rat TyrH activity was inhibited by DDC from *Pseudomonas putida* **[39]**. In our
334 experiment, mouse TyrH activity was likely inhibited by pig DDC. We need further
335 analysis to elucidate this inhibition effect to improve productivity.

336 Effective DOPA-producing pathways in microbial cells have garnered much
337 attention for fermentative production of natural plant products, such as the
338 benzylisoquinoline alkaloids, morphine and codeine, and the pigment betalains **[39–42]**.
339 For benzylisoquinoline alkaloid production, a tyrosinase has been used to produce DOPA
340 from Tyr. The enzyme catalyzes multiple oxidation reactions, including Tyr to DOPA and
341 DOPA to *ortho*-quinone, using molecular oxygen. This overoxidation results in low
342 product yield. In contrast, the yield has been improved by utilization of monooxygenase

343 TyrH from *Drosophila melanogaster,* overcoming the overoxidation issue of tyrosinase.
344 Therefore, TyrHs are widely applicable for development of microbial cell factories that
345 can produce various DOPA derivatives. Since the accumulation of Tyr (4.61 mM) was
346 detected under our experimental conditions, as shown in Figure 7A, we need to optimize
347 the cultivation conditions and/or search for and engineer more active enzymes for
348 increased production of DOPA.

349 To facilitate engineering of microbial cell factories in a high-throughput fashion,
350 Design–Build–Test–Learn cycles can be applied for optimization and fine-tuning of the
351 designed biosynthetic pathways. In these cycles, combinatorial DNA parts, consisting of
352 the relevant genes with promoters of different strength, ribosome binding sites of different
353 translation efficiency, and artificial operons in various gene orders, are constructed,
354 introduced into the microbial cells, and evaluated in parallel. The key cultivation
355 parameters are monitored in real time using optical measurement systems **[43]**. Recent
356 advancements in *in vivo* biosensors, used to evaluate the concentration of products and
357 intermediates, coupled to fluorescence proteins, which produce a real-time output signal,
358 make the optical measurement more sensitive and reliable. However, Tyr precipitates
359 would interfere with these optical measurements, owing to the addition of the reactant to
360 the medium at high concentrations. In contrast, the platform strains preventing the issue

would accelerate the efficient development of microbial cell factories.

Our ultimate goal was the development of microbial cell factories to produce Tyr-derivatives from renewable resources of biomass. To achieve this, the pathways (modules), optimized by our platform strains, can be installed into strains already engineered for Tyr-overproduction from biomass. Phe-overproducing strains can also be employed by installing the pathways (modules) together with PheH and a BH4-regeneration system. In fact, Huang *et al*. reported production of 2.21 mM (0.401 g/L) Tyr by a strain overexpressing a bacterial PheH gene, as well as genes responsible for the shikimate pathway and MH4 biosynthesis and recycling **[44].** The Phe producers with a PheH may have advantages over Tyr producers, because the Phe titer of engineered strains (over 6 g/L) is higher than the Tyr titer of Tyr producers **[45, 46]**. In addition, some Tyr producers are *pheA* knockout mutants (Phe auxotrophy) due to the increased metabolic flux toward Tyr from chorismate and require Phe supplementation **[18]**. Conversely, Phe producers with PheH do not require Phe supplementation. As another approach, we would employ modular co-culture metabolic engineering approach **[47–49]**. In this case, the strains with Tyr-derivative-producing module(s) produce appropriate compounds using Phe, which is biosynthesized from biomass by the Phe producer, under co-culture conditions.

Remarkable progress of Clustered Regularly Interspaced Short Palindromic Repeats (CRISPR)/CRISPR-associated protein (Cas) technology in recent years has vastly facilitated genome editing of various organisms, including prokaryotes and eukaryotes. This technology is also now used widely for chromosome engineering to develop metabolic engineered strains **[11, 50]**. Compared to the described method that uses λRed recombinase, CRISPR/Cas technology allows for more flexible scarless integration of a DNA fragment into the chromosome. However, this system poses the risk of off-target effects, which induces mutation at untargeted sites. To reduce this unwanted effect, selection of appropriate CRISPR/Cas tools and careful design of a guide-RNA sequence are needed. Taking this into account, the scarless gene integration method based on the commonly used λRed recombination would be advantageous.

CONCLUSIONS

In this study, we developed simple and convenient Tyr-producing *E. coli* platforms, which employ a bacterial PheH and a human BH4-regeneration system, using endogenous MH4 as a cofactor. These platforms produced Tyr in multi-gram-per-liter levels from Phe supplemented as the substrate. These platforms allowed development and evaluation of various designed Tyr-derivative biosynthetic pathways. The usefulness of

the platforms was demonstrated using DOPA, tyrosol, and hydroxytyrosol production as examples. Furthermore, to facilitate development of chromosome engineering strains for metabolic engineering, we showed a scarless gene integration method based on the well-established λRed recombineering system combined with complementation of auxotrophic phenotypes.

MATERIALS AND METHODS

General

All media, chemicals, and reagents were of analytical grade and were purchased from FUJIFILM Wako Pure Chemical Corporation (Osaka, Japan), Sigma-Aldrich Japan K.K. (Tokyo, Japan), KANTO CHEMICAL Co., Inc. (Tokyo, Japan), or Tokyo Chemical Industry Co., Ltd. (Tokyo, Japan). Synthetic genes were purchased from Integrated DNA Technologies, Inc. (Coralville, IA, USA). PCR was performed using a GeneAmp PCR System 9700 thermal cycler (Thermo Fisher Scientific Inc., Waltham, MA, USA) with KOD DNA polymerase (Toyobo Co. Ltd, Osaka, Japan) according to the manufacturer's protocols. General genetic manipulations of *E. coli* were performed according to standard protocols.

Bacterial strains and cultures

The strains used in this study are summarized in Table 2. *Escherichia coli* JM109 (Nippon Gene Co., Ltd, Tokyo, Japan) was routinely used for plasmid construction. For Tyr production, *E. coli* BW25113 derivatives were used.

The growth medium routinely used was LB broth medium (Lennox; Sigma-Aldrich Japan K.K.). M9 minimal medium [M9 minimal salts (Becton, Dickinson and Company, Franklin Lakes, NJ, USA), 0.4 or 1.0%(w/v) carbon sources (glucose or glycerol), 5 mM $MgSO_4$, 0.1 mM $CaCl_2$] supplemented with 0.1%(w/v) yeast extract (M9Y medium) was used for Tyr production. Ampicillin (Ap), chloramphenicol (Cm), streptomycin (Sm), and kanamycin (Km) were added to media at 100, 30, 20, and 25 mg/L, respectively, to maintain plasmids. For the selection of gene knockout mutants, Km was used at 13 mg/L.

Plasmid construction

Plasmids used in this study are listed in Table 1 and Figure 1B. Detailed methods for plasmid construction are described in the supplementary materials.

Production of Tyr and its derivatives.

Escherichia coli strains harboring appropriate plasmids were pre-cultured in M9Y

433 medium containing 0.4%(w/v) glucose or glycerol for 16 h at 30 °C. After inoculating
434 appropriate amounts of the precultures into 3 mL of M9Y medium so that optical density
435 (OD) at 600 nm to 0.15, they were incubated at 30 °C with shaking (200 rpm). The
436 medium contained 5.00 g/L (30.3 mM) Phe, 20 mg/L $FeSO_4 \cdot 7H_2O$, and 10 g/L
437 (1.0%[w/v]) of the same carbon sources used for pre-cultivation with test tubes. To induce
438 protein expression, IPTG was added to a final concentration of 500 μM at 4 h of
439 cultivation, unless noted otherwise. Samples (300 μL) were collected at appropriate time-
440 points and were analyzed by HPLC. OD measurements at 600 nm were also taken using
441 a NanoDrop 2000C spectrophotometer (Thermo Fisher Scientific Inc.), using cuvettes
442 after dilution in a 1 N HCl solution.
443
444 ***HPLC analysis***
445 Culture aliquots (50 μL) mixed with 1 N HCl (200 μL) were heated at 50 °C for 30
446 min. After centrifugation, the supernatants (2 μL) were analyzed using a Shimadzu HPLC
447 system (Shimadzu Co., Kyoto, Japan), equipped with an InertSustain C18 column
448 (column length, 150 mm; inner diameter, 2.1 mm; particle size, 3 μm; GL Science Inc.,
449 Tokyo, Japan). Buffer A (0.1%[v/v] formic acid solution) and buffer B (methanol with
450 0.1%[v/v] formic acid) were used as a mobile phase, and compounds were eluted at 35 °C

and a flow rate of 0.2 mL/min, with increasing concentrations of buffer B as follows: 2%, 0−3 min; 2–30%, 3–35 min. Eluted compounds were detected by measuring absorbance at 210 and 280 nm.

LIST OF ABBREVIATIONS

Ap, Ampicillin

BH4, tetrahydrobiopterin

Cas, CRISPR-associated protein

Cm, chloramphenicol

CRISPR, clustered regularly interspaced short palindromic repeats

DHPR, dihydropteridine reductase

DOPA, 3,4-dihydroxyphenylalanine

FLP, flippase

FRT, flippase recognition target

HPAAld, 4-hydroxyphenylacetaldehyde

HPLC, high-performance liquid chromatography

IPTG, isopropyl-β-D-thiogalactopyranoside

Km, kanamycin

MH4, tetrahydromonapterin

OD, optical density

PCD, pterin-4α-carbinolamine dehydratase

Phe, phenylalanine

PheH, phenylalanine hydroxylase

qMH2, quinonoid dihydromonapterin

RatPheH, rat phenylalanine hydroxylase

RatPheHc, catalytic domain of rat phenylalanine hydroxylase

Sm, streptomycin

TDC, tyrosine decarboxylase

Trp, tryptophan

TYO, tyramine oxidase

Tyr, tyrosine

TyrH, tyrosine hydroxylase

SUPPLEMENTARY INFORMATION

The online version contains supplementary material available at xxx.

DECLARATIONS

Ethics approval and consent to participate

Not applicable

Consent for publication

Not applicable

Availability of data and materials

All data generated or analyzed during this study are included in this published article and its supplementary information files.

Competing interests

The authors declare that they have no competing interests.

Funding

This work was supported by JSPS KAKENHI Grant Number JP16K06864 and JP22K04835 to Y.S. This work was also granted from ENEOS TONENGENERAL Research/Development Encouragement & Scholarship Foundation, KOSÉ Cosmetology

Research Foundation, and The Akiyama Life Science Foundation to Y.S. N.S. was supported by Hokkaido University Ambitious Doctoral Fellowship by the Ministry of Education, Culture, Sports, Science and Technology (MEXT).

Authors' contributions

Yasuharu Satoh: Conceptualization, Methodology, Investigation, Visualization, Writing – Original Draft, Writing – Review & Editing.

Keita Fukui: Conceptualization, Methodology, Writing – Review & Editing.

Daisuke Koma: Methodology, Investigation, Writing – Review & Editing.

Ning Shen: Validation.

Taek Soon Lee: Methodology, Writing – Review & Editing.

Acknowledgement

We would like to thank Professor Tohru Dairi (Hokkaido University) for valuable discussions.

REFERENCES

1. Averesch NJH, Krömer JO. Metabolic engineering of the shikimate pathway for

production of aromatics and derived compounds–present and future strain construction strategies. Front Bioeng Biotechnol. 2018;6:32.

2. Cao M, Gao M, Suástegui M, Mei Y, Shao Z. Building microbial factories for the production of aromatic amino acid pathway derivatives: from commodity chemicals to plant-sourced natural products. Metab Eng. 2020;58:94–132.

3. Thompson B, Machas M, Nielsen DR. Creating pathways towards aromatic building blocks and fine chemicals. Curr Opin Biotechnol. 2015;36:1–7.

4. Shen YP, Niu FX, Yan ZB, Fong LS, Huang YB, Liu JZ. Recent advances in metabolically engineered microorganisms for the production of aromatic chemicals derived from aromatic amino acids. Front Bioeng Biotechnol. 2020;8:407.

5. Yang D, Park SY, Park YS, Eun H, Lee SY. Metabolic engineering of Escherichia coli for natural product biosynthesis. Trends Biotechnol. 2020;38:745–65.

6. Robinson CJ, Carbonell P, Jervis AJ, Yan C, Hollywood KA, Dunstan MS, Currin A, Swainston N, Spiess R, Taylor S et al. Rapid prototyping of microbial production strains for the biomanufacture of potential materials monomers. Metab Eng. 2020;60:168–82.

7. Nielsen J, Tillegreen CB, Petranovic D. Innovation trends in industrial

biotechnology. Trends Biotechnol. 2022;40:1160–72.

8. Keasling J, Garcia Martin H, Lee TS, Mukhopadhyay A, Singer SW, Sundstrom E. Microbial production of advanced biofuels. Nat Rev Microbiol. 2021;19:701–15.

9. Xu X, Liu Y, Du G, Ledesma-Amaro R, Liu L. Microbial chassis development for natural product biosynthesis. Trends Biotechnol. 2020;38:779–96.

10. Choi KR, Jang WD, Yang D, Cho JS, Park D, Lee SY. Systems metabolic engineering strategies: integrating systems and synthetic biology with metabolic engineering. Trends Biotechnol. 2019;37:817–37.

11. Ko YS, Kim JW, Lee JA, Han T, Kim GB, Park JE, Lee SY. Tools and strategies of systems metabolic engineering for the development of microbial cell factories for chemical production. Chem Soc Rev. 2020;49:4615–36.

12. Satoh Y, Tajima K, Munekata M, Keasling JD, Lee TS. Engineering of a tyrosol-producing pathway, utilizing simple sugar and the central metabolic tyrosine, in Escherichia coli. J Agric Food Chem. 2012;60:979–84.

13. Satoh Y, Tajima K, Munekata M, Keasling JD, Lee TS. Engineering of L-tyrosine oxidation in Escherichia coli and microbial production of hydroxytyrosol. Metab Eng. 2012;14:603–10.

559 14. Rodriguez A, Martínez JA, Flores N, Escalante A, Gosset G, Bolivar F.
560 Engineering Escherichia coli to overproduce aromatic amino acids and derived
561 compounds. Microb Cell Fact. 2014;13:126.
562 15. Zimmer A, Mueller R, Wehsling M, Schnellbaecher A, von Hagen J. Improvement
563 and simplification of fed-batch bioprocesses with a highly soluble
564 phosphotyrosine sodium salt. J Biotechnol. 2014;186:110–8.
565 16. Juminaga D, Baidoo EE, Redding-Johanson AM, Batth TS, Burd H,
566 Mukhopadhyay A, Petzold CJ, Keasling JD. Modular engineering of L-tyrosine
567 production in Escherichia coli. Appl Environ Microbiol. 2012;78:89–98.
568 17. Kim SC, Min BE, Hwang HG, Seo SW, Jung GY. Pathway optimization by re-
569 design of untranslated regions for L-tyrosine production in Escherichia coli. Sci
570 Rep. 2015;5:13853.
571 18. Koma D, Kishida T, Yoshida E, Ohashi H, Yamanaka H, Moriyoshi K, Nagamori
572 E, Ohmoto T. Chromosome engineering to generate plasmid-free phenylalanine-
573 and tyrosine-overproducing Escherichia coli strains that can be applied in the
574 generation of aromatic-compound-producing bacteria. Appl Environ Microbiol.
575 2020;86:e00525-20.
576 19. Daubner SC, Hillas PJ, Fitzpatrick PF. Characterization of chimeric pterin-

577 dependent hydroxylases: contributions of the regulatory domains of tyrosine and
578 phenylalanine hydroxylase to substrate specificity. Biochemistry 1997;36:11574–
579 82.
580 20. Flydal MI, Martinez A. Phenylalanine hydroxylase: function, structure, and
581 regulation. IUBMB Life 2013;65:341–9.
582 21. Onishi A, Liotta LJ, Benkovic SJ. Cloning and expression of Chromobacterium
583 violaceum phenylalanine hydroxylase in Escherichia coli and comparison of
584 amino acid sequence with mammalian aromatic amino acid hydroxylases. J Biol
585 Chem. 1991;266:18454–9.
586 22. Pribat A, Blaby IK, Lara-Núñez A, Gregory 3rd JF, de Crécy-Lagard V, Hanson
587 AD. FolX and FolM are essential for tetrahydromonapterin synthesis in
588 Escherichia coli and Pseudomonas aeruginosa. J Bacteriol. 2010;192:475–82.
589 23. Daubner SC, Melendez J, Fitzpatrick PF. Reversing the substrate specificities of
590 phenylalanine and tyrosine hydroxylase: aspartate 425 of tyrosine hydroxylase is
591 essential for L-DOPA formation. Biochemistry 2000;39:9652–61.
592 24. Baba T, Ara T, Hasegawa M, Takai Y, Okumura Y, Baba M, Datsenko KA, Tomita
593 M, Wanner BL, Mori H. Construction of Escherichia coli K-12 in-frame, single-
594 gene knockout mutants: the Keio collection. Mol Syst Biol. 2006;2:2006.0008.

595 25. da Silva GP, Mack M, Contiero J. Glycerol: a promising and abundant carbon
596 source for industrial microbiology. Biotechnol Adv. 2009;27:30–9.
597 26. Tajima K, Igari T, Nishimura D, Nakamura M, Satoh Y, Munekata M. Isolation
598 and characterization of Bacillus sp. INT005 accumulating polyhydroxyalkanoate
599 (PHA) from gas field soil. J Biosci Bioeng. 2003;95:77–81.
600 27. Yoo S. Antihypertensive polyhalohydroxyisopropyl phenylalka(e)noic acid esters
601 of alkylaminohydroxypropyloxyphenylalkyl alcohols. U.S. Patent 1984;4450172.
602 28. Ippolito RM, Vigmond S. Process for preparing substituted phenol ethers via
603 oxazolidine-structure intermediates. U.S. Patent 1988;4760182.
604 29. Granado L, Tavernier R, Henry S, Auke RO, Foyer G, David G, Caillol S. Toward
605 sustainable phenolic thermosets with high thermal performances. ACS Sustain
606 Chem Eng. 2019;7:7209–17.
607 30. Santos CNS, Regitsky DD, Yoshikuni Y. Implementation of stable and complex
608 biological systems through recombinase-assisted genome engineering. Nat
609 Commun. 2013;4:2503.
610 31. Datsenko KA, Wanner BL. One-step inactivation of chromosomal genes in
611 Escherichia coli K-12 using PCR products. Proc Natl Acad Sci U S A.
612 2000;97:6640–5.

613 32. Sawitzke JA, Thomason LC, Costantino N, Bubunenko M, Datta S, Court DL.
614 Recombineering: in vivo genetic engineering in E. coli, S. enterica, and Beyond.
615 Methods Enzymol. 2007;421:171–99.
616 33. Sharan SK, Thomason LC, Kuznetsov SG, Court DL. Recombineering: a
617 homologous recombination-based method of genetic engineering. Nat Protoc.
618 2009;4:206–23.
619 34. Satoh Y, Kuratsu M, Kobayashi D, Dairi T. New gene responsible for para-
620 aminobenzoate biosynthesis. J Biosci Bioeng. 2014;117:178–83.
621 35. Di Luca DG, Reyes NGD, Fox SH. Newly approved and investigational drugs for
622 motor symptom control in Parkinson's Disease. Drugs 2022;82:1027–53.
623 36. Omar SH: Oleuropein in olive and its pharmacological effects. Sci Pharm.
624 2010;78:133–54.
625 37. Martínez-Zamora L, Peñalver R, Ros G, Nieto G. Olive tree derivatives and
626 hydroxytyrosol: their potential effects on human health and its use as functional
627 ingredient in meat. Foods 2021;10:2611.
628 38. Blechingberg J, Holm IE, Johansen MG, Børglum AD, Nielsen AL. Aromatic L-
629 amino acid decarboxylase expression profiling and isoform detection in the
630 developing porcine brain. Brain Res. 2010;1308:1–13.

631 39. Nakagawa A, Nakamura S, Matsumura E, Yashima Y, Takao M, Aburatani S, Yaoi
632 K, Katayama T, Minami H. Selection of the optimal tyrosine hydroxylation
633 enzyme for (S)-reticuline production in Escherichia coli. Appl Microbiol
634 Biotechnol. 2021;105:5433–47.
635 40. Galanie S, Thodey K, Trenchard IJ, Filsinger Interrante M, Smolke CD. Complete
636 biosynthesis of opioids in yeast. Science 2015;349:1095–100.
637 41. Grewal PS, Modavi C, Russ ZN, Harris NC, Dueber JE. Bioproduction of a
638 betalain color palette in Saccharomyces cerevisiae. Metab Eng. 2018;45:180–8.
639 42. Matsumura E, Nakagawa A, Tomabechi Y, Ikushiro S, Sakaki T, Katayama T,
640 Yamamoto K, Kumagai H, Sato F, Minami H. Microbial production of novel
641 sulphated alkaloids for drug discovery. Sci Rep. 2018;8:7980.
642 43. Hemmerich J, Noack S, Wiechert W, Oldiges M. Microbioreactor systems for
643 accelerated bioprocess development. Biotechnol J. 2018;13:1700141.
644 44. Huang J, Lin Y, Yuan Q, Yan Y. Production of tyrosine through phenylalanine
645 hydroxylation bypasses the intrinsic feedback inhibition in Escherichia coli. J Ind
646 Microbiol Biotechnol. 2015;42:655–9.
647 45. Zhou H, Liao X, Wang T, Du G, Chen J. Enhanced L-phenylalanine biosynthesis
648 by co-expression of $pheA^{fbr}$ and $aroF^{wt}$. Bioresour Technol. 2010;101:4151–6.

649 46. Wu WB, Guo XL, Zhang ML, Huang QG, Qi F, Huang JZ. Enhancement of L-
650 phenylalanine production in Escherichia coli by heterologous expression of
651 Vitreoscilla hemoglobin. Biotechnol Appl Biochem. 2018;65:476–83.
652 47. Zhang H, Wang X. Modular co-culture engineering, a new approach for metabolic
653 engineering. Metab Eng. 2016;37:114–21.
654 48. Liu X, Li XB, Jiang J, Liu ZN, Qiao B, Li FF, Cheng JS, Sun X, Yuan YJ, Qiao J
655 et al. Convergent engineering of syntrophic Escherichia coli coculture for efficient
656 production of glycosides. Metab Eng. 2018;47:243–53.
657 49. Wang R, Zhao S, Wang Z, Koffas MAG. Recent advances in modular co-culture
658 engineering for synthesis of natural products. Curr Opin Biotechnol. 2020;62:65–
659 71.
660 50. Jakočiūnas T, Jensen MK, Keasling JD. CRISPR/Cas9 advances engineering of
661 microbial cell factories. Metab Eng. 2016;34:44–59.
662
663

664 **FIGURE CAPTIONS**

665 **Figure 1. Biosynthetic pathways for producing tyrosine and its derivatives from**
666 **phenylalanine (A) and gene organization in the constructed plasmids (B).**

667

668 **Figure 2. Tyrosine production of plasmid-based engineered strains with Rat**
669 **pheylalanine hydroxyase.**

670 Strain YBR expressing the catalytic domain of RatPheH (RatPheHc), using glucose (A)
671 or glycerol (B) as the carbon sources. Each of the transformants was cultured up to 48 h
672 at 30 °C. Phe, black squares; Tyr, blue squares; OD, white circles. Data are presented as
673 mean values with standard deviations for three independent experiments. Symbols
674 without an error bar indicate that they are larger than the size of the error bar.

675

676 **Figure 3. Tyrosine production of plasmid-based engineered strains with bacterial**
677 **phenylalanine hydroxylases.**

678 (A) Tyrosine production of strain YBR harboring pQE1a derivatives, including bacterial
679 PheHs. Each of the transformants was cultured for 48 h at 30 °C. Glycerol was used as
680 the carbon source. BsPheH, Bs; CnPheH, Cn; CvPheH, Cv; GsPheH1, Gs1; GsPheH2,
681 Gs2; XoPheH, Xo; PpPheH, Pp; OD, circles; Tyr, bars. (B and C) Fermentation profiles

682 of tyrosine production of strain YBR harboring pQE1a-Gs1 (B) and strain PGs (C). Each
683 of the transformants was cultured up to 48 h at 30 °C. Phe, black squares; Tyr, blue
684 squares; OD, white circles. Data are presented as mean values with standard deviations
685 for three independent experiments. Symbols without an error bar indicate that they are
686 larger than the size of the error bar.
687
688 **Figure 4. Tyrosol production of plasmid-based engineered strains.**
689 Fermentation profiles of tyrosol production of strain PGs harboring pCF1s-TDC-TYO
690 (A) or pCF1s-TYO-TDC (B). Each of the transformants was cultured up to 72 h at 30 °C.
691 Phe, black squares; Tyr, blue squares; tyramine, orange triangles; tyrosol, red triangles;
692 OD, white circles. Data are presented as mean values with standard deviations for three
693 independent experiments. Symbols without an error bar indicate that they are larger than
694 the size of the error bar.
695
696 **Figure 5. Tyrosine production of chromosome engineered strains GsBR1 to GsBR5.**
697 Strains GsBR1 (white), GsBR2 (gray), GsBR3 (orange), GsBR4 (green), and GsBR5
698 (yellow), in which one to five Tyr-producing modules were integrated at different gene
699 loci on the chromosome, were tested. Strains GsBR1, GsBR3, and GsBR5 transformed

700 with pQE1a-Gs1 (GsPheH1) or pSTV-BH4R (BH4R) were also evaluated. Each strain
701 was cultured for 48 h at 30 °C. Tyr, bars; OD, blue circles. Data are presented as mean
702 values with standard deviations for three independent experiments. Symbols without an
703 error bar indicate that they are larger than the size of the error bar.
704
705 **Figure 6. Schematic diagram of scarless chromosome engineering using λRed**
706 **recombinase.**
707 Schematic diagram of scarless chromosome engineering. First, an auxotrophic mutant
708 with an essential gene knocked out is constructed using λRed recombinase and an
709 antibiotic-resistance marker. The auxotrophic phenotype of the mutant is then recovered
710 using λRed recombinase and a DNA fragment in which the essential gene and a target
711 module are assembled by overlap extension polymerase chain reaction.
712
713 **Figure 7. DOPA and tyrosol production of chromosome engineered strain GsBR5.**
714 DOPA (A) and tyrosol (B) production of recombinant GsBR5. Strain GsBR5 was
715 transformed with pBbE1k-3 for DOPA production and pCF1s-TDC-TYO-BH4R for
716 tyrosol production, respectively. Each strain was cultured up to 72 h at 30 °C. Phe, black
717 squares; Tyr, blue squares; DOPA, purple diamonds; tyramine, orange triangles; tyrosol,

718 red triangles; OD, white circles. Data are presented as mean values with standard
719 deviations for three independent experiments. Symbols without an error bar indicate that
720 they are larger than the size of the error bar.
721
722 **Figure 8. Hydroxytyrosol production of chromosome engineered strain GsBR5.**
723 Hydroxytyrosol production of recombinant GsBR5 transformed with pBbE1k-3 and
724 pBbS1a-3. The recombinant cell, treated at different IPTG concentration to induce target
725 protein production, was cultured up to 96 h at 30 °C. Data are presented as mean values
726 with standard deviations for three independent experiments. Symbols without an error bar
727 indicate that they are larger than the size of the error bar.
728

729 Figure 1

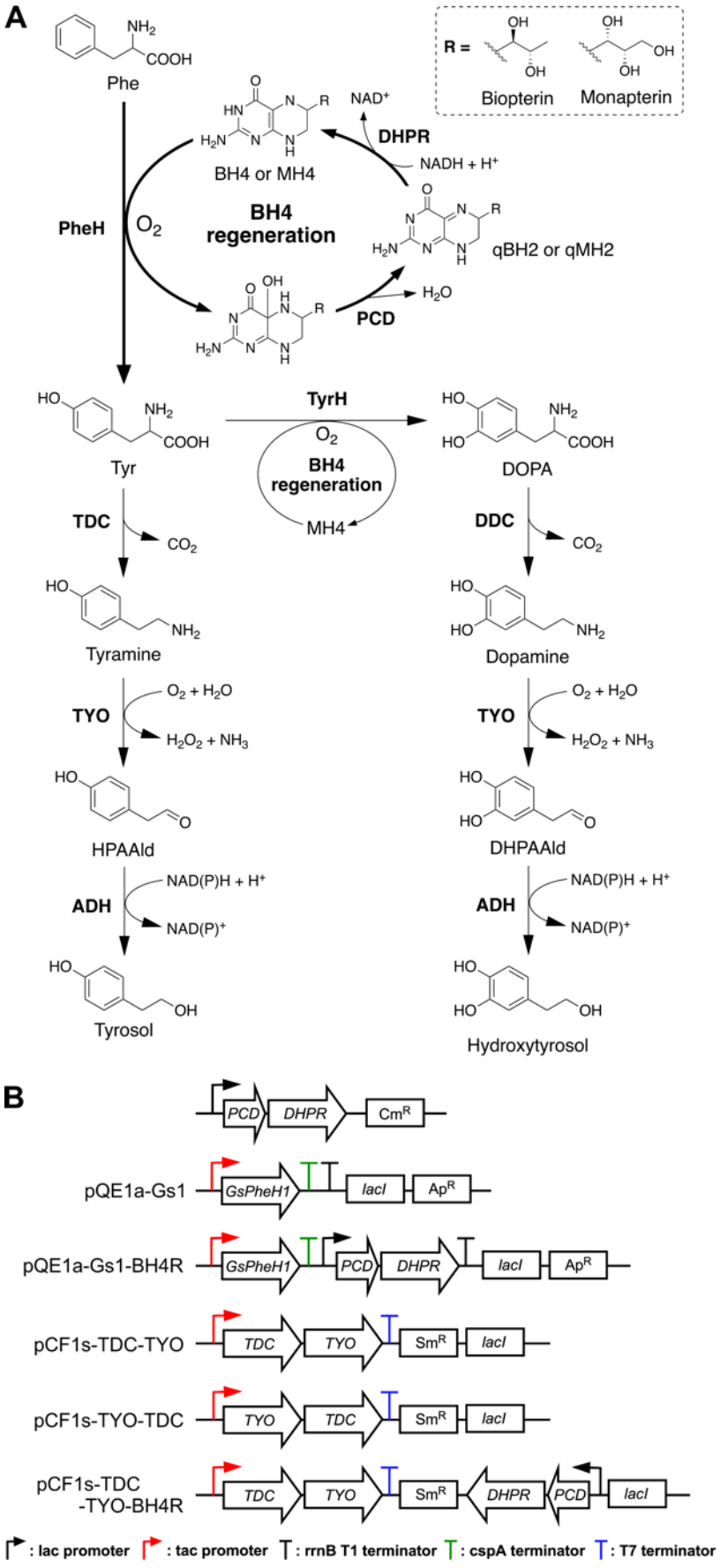
A
Phe
PheH
O2
BH4 or MH4
BH4 regeneration
NAD+
DHPR
NADH + H+
qBH2 or qMH2
PCD
H2O
R =
Biopterin
Monapterin
Tyr
TyrH
O2
BH4 regeneration
MH4
DOPA
TDC
CO2
DDC
CO2
Tyramine
Dopamine
TYO
O2 + H2O
H2O2 + NH3
TYO
O2 + H2O
H2O2 + NH3
HPAAld
DHPAAld
ADH
NAD(P)H + H+
NAD(P)+
ADH
NAD(P)H + H+
NAD(P)+
Tyrosol
Hydroxytyrosol
B
PCD
DHPR
CmR
pQE1a-Gs1
GsPheH1
lacI
ApR
pQE1a-Gs1-BH4R
GsPheH1
PCD
DHPR
lacI
ApR
pCF1s-TDC-TYO
TDC
TYO
SmR
lacI
pCF1s-TYO-TDC
TYO
TDC
SmR
lacI
pCF1s-TDC
-TYO-BH4R
TDC
TYO
SmR
DHPR
PCD
lacI
: lac promoter
: tac promoter
: rrnB T1 terminator
: cspA terminator
: T7 terminator

730 Figure 2

731

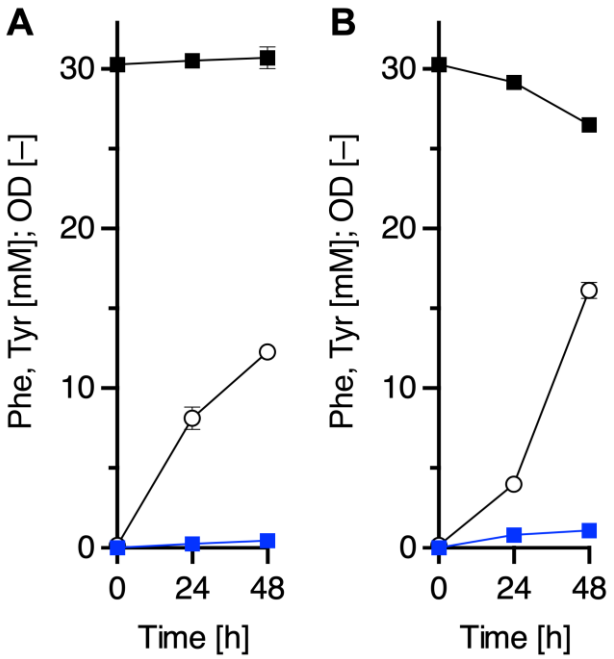

732

733

734 Figure 3

735

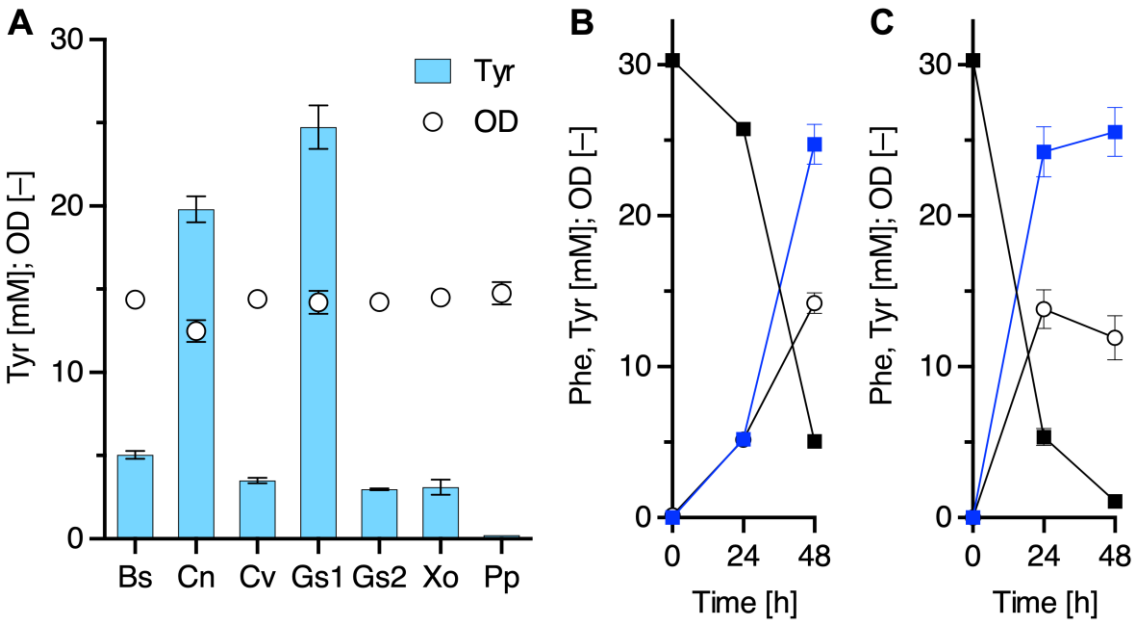

736

737

738 Figure 4

739

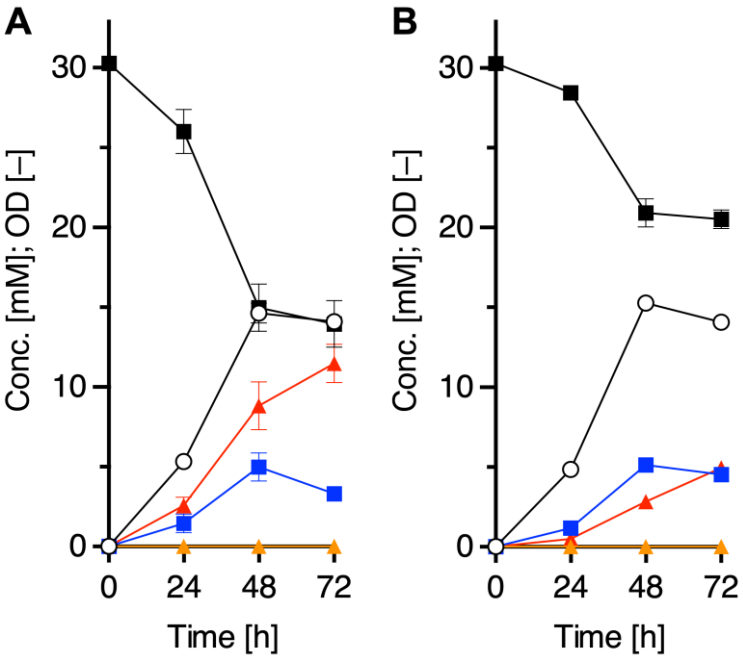

740

741

742 Figure 5

743

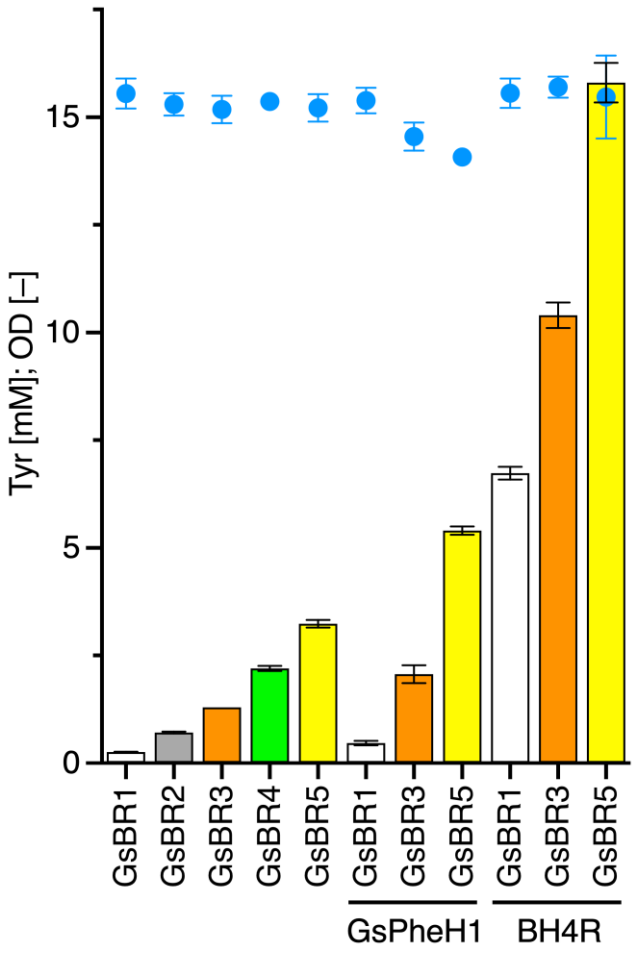

744

745

746 Figure 6

747

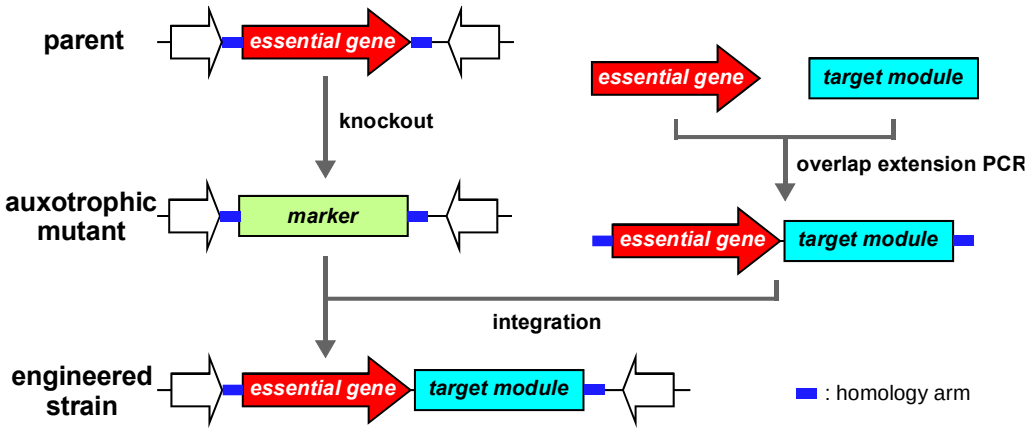

748

749

Figure 7

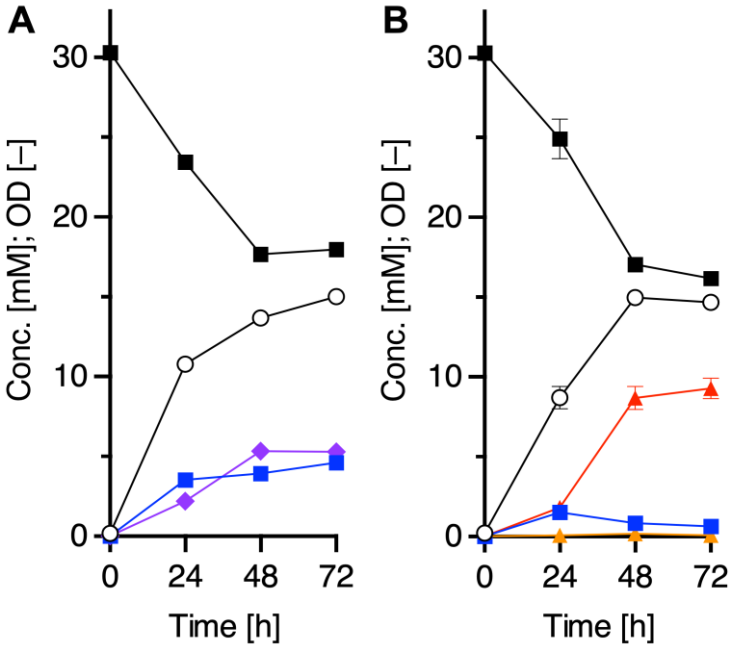

753 Figure 8

754

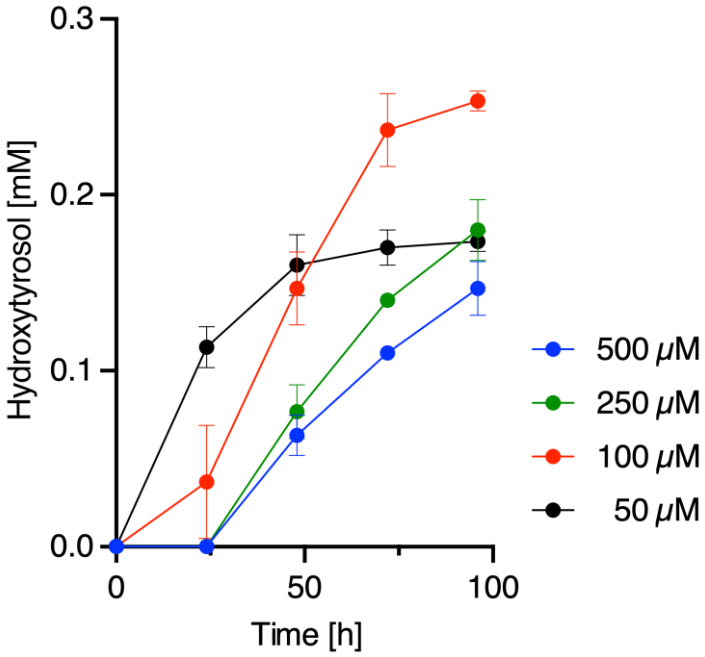

755

756